chemosensors

Article

Reliability of Sensors Based on Nanowire Networks When the Electrical Current is Allowed to Move in All Directions

Nader Ebrahimi [1] and Kristin McCullough [2],*

[1] Division of Statistics, Northern Illinois University, DeKalb, IL 60115, USA;
E-Mail: nader@math.niu.edu

[2] Department of Mathematics, Grand View University, Des Moines, IA 50316, USA

* Author to whom correspondence should be addressed; E-Mail: kmccullo4@gmail.com;
Tel.: +515-263-6176.

Abstract: Nanowire networks have great potential in many industrial applications, including batteries, electrical circuits, solar cells, and sensors. In this paper we focus on a specific hydrogen gas nanosensor whose sensing element is a network of palladium nanowires. The nanosensor is modeled using a square, equilateral triangle, and hexagonal lattice. We provide the reliability behavior of this nanosensor when the electrical current is allowed to move in all directions. Our findings reveal an improvement in reliability compared to the scenario where the electrical current could not move from right to left. We show this improvement both analytically and through simulation.

Keywords: nanosensor; nanowire; reliability; reliability growth; percolation; lattice

1. Introduction

Due to their large surface area to volume ratio and available space for making electrical contacts, nanowires have been utilized as interconnects or sensing elements in nanodevices. Nanosensors composed of a single nanowire show improvements in speed, sensitivity, and ultra-low power consumption in comparison to thin or thick film sensors [1–3]. However, the utilization of an individual nanowire creates challenges for fabrication and manipulation. A single nanowire also has a high probability of being broken in an application environment, as demonstrated by Yang *et al*. [4].

Using a network of nanowires has the same advantages as using individual nanowires without the fabrication and performance obstacles.

We focus on a specific network of ultra-small palladium (Pd) nanowires used as the sensing element in a hydrogen gas (H_2) nanosensor. The network is created using the fabrication process presented in [1]. Figure 1 shows a top-view scanning electron microscopy (SEM) image of said network. Electrical contacts are placed on opposite ends, and an electrical current is passed through to monitor the resistivity of the Pd. When H_2 is introduced the nanowires swell and adsorb the H_2 creating Pd hydride, which has a higher resistivity than pure Pd. The nanowires decrease in volume when the H_2 is purged. During this process, which we call a cycle of hydrogen gas, the Pd atoms move around causing nanoscopic gaps to form in various nanowires [1]. We consider a nanowire with a gap to be permanently broken, and we are interested in how long the nanosensor can withstand such damage.

Figure 1. SEM image of a network of palladium (Pd) nanowires with a deposition thickness of 7 nanometers.
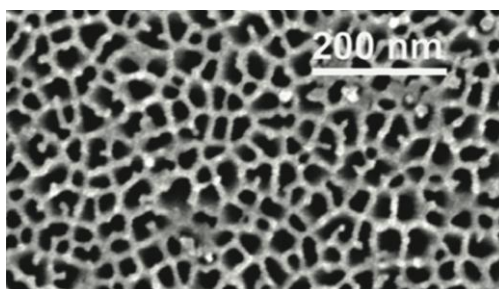

We define the lifetime of the nanosensor to be the number of cycles of H_2 that the nanosensor withstands before the electrical current can no longer make it from the left electrical contact to the right electrical contact. It is natural then to define the reliability in terms of several checks for percolation, where each check occurs after a cycle of hydrogen gas. For our nanosensor the electrical current will always prioritize moving left to right in order to follow the path of least resistance and obey Kirchoff's Laws. Although they are unlikely, certain nanowire configurations occur where the electrical current must flow from right to left in order to percolate. This paper extends the work in [5–7], where we limited the electrical current to only left to right movement, to the scenario where the current can move in all directions. This work also compares the reliability of our nanosensor under these two scenarios.

We continue to use the square lattice (SL), equilateral triangle lattice (ETL), and hexagonal lattice (HL) to model the structure of the network. Examples of these three structures can be seen in Figure 2. Although we are simplifying the structure for the purpose of theoretical modeling, such networks can be actualized by using the self-assembled nanoporous anodisc alumina membranes from [8] in the nanofabrication approach presented in [1–3]. Thus the results developed in this paper are applicable to other nanodevices that have a similar structure to our nanosensor or have SL, ETL, or HL structure.

As in [5–7] we use two models to describe the probability of a nanowire in the network not breaking. We define p_i to be the probability of a nanowire not breaking during cycle i, $i = 1,2,3,...$ In Model 1 the probability of a nanowire not breaking remains the same over all cycles of H_2, *i.e.*,

$p_1=p_2=...=p$. In model 2 the nanosensor is operating in a dynamic environment, which we define to be any scenario in which the probability of a nanowire not breaking changes over cycles of hydrogen gas. A special case of this model was considered in Ebrahimi *et al.* [6] where the nanosensor was operating under uniform decay conditions.

Figure 2. Functioning nanosensors with (**a**) square lattice (SL), (**b**) equilateral triangle lattice (ETL), and (**c**) hexagonal lattice (HL) structures. The nanowires which are not shown are considered to have broken.

(**a**)   (**b**)   (**c**)
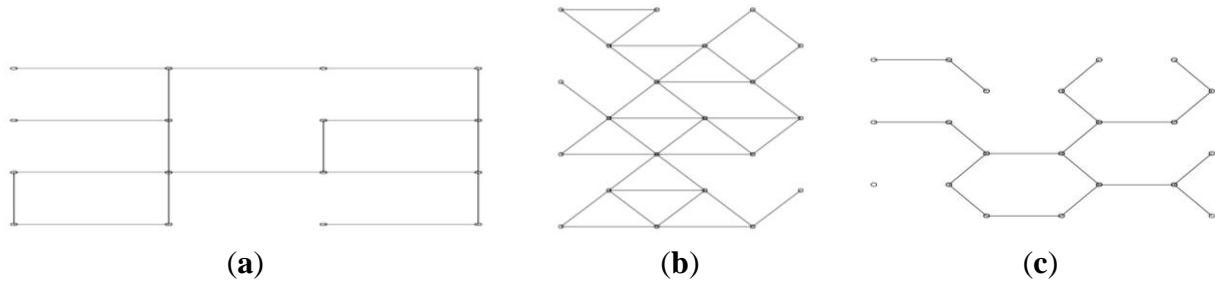
This paper is organized as follows. In Section 2, we discuss the reliability of our nanosensor under both nanowire probability models using the assumption that the electrical current can move in all directions. We show that there is an increase in reliability compared to the results obtained in Ebrahimi *et al.* [5–7] where movement was restricted. In Section 3, we present theoretical properties describing this reliability growth. Concluding remarks are in Section 4.

2. Assessing the Reliability of Nanosensors

In this section we assess the reliability of our nanosensor under both nanowire probability models. First we define $n \times m$ to be the size of the nanosensor. For all lattice types n and m refer to the number of vertices that could potentially be in the row and column, respectively. For a nanosensor of size $n \times m$ we define $X_{n \times m}$, $X^E_{n \times m}$, and $X^H_{n \times m}$ to be the random variables that represent the number of cycles of H_2 that a nanosensor with SL, ETL, and HL structure, respectively, will last through before they no longer percolate. We then define $R_{n \times m}(x)$, $R^E_{n \times m}(x)$, and $R^H_{n \times m}(x)$ to be the reliability functions for nanosensors with SL, ETL, and HL structure, respectively. Similarly, $E(X_{n \times m})$, $E(X^E_{n \times m})$, and $E(X^H_{n \times m})$ are the expected lifetimes.

2.1. Model 1: $p_1=p_2=...=p$

In [5] and [7] the authors presented exact formulas for the reliability functions and expected lifetimes of $2 \times m$ nanosensors with SL structure, $3 \times m$ nanosensors with ETL structure, and $4 \times m$ nanosensors with HL structure when the movement of the electrical current was restricted. These formulas still hold when the electrical current can move in all directions, because percolation on these specific structures does not benefit from the electrical current being able to move right to left. Specifically for $2 \times m$ nanosensors with SL structure and $4 \times m$ nanosensors with HL structure, right to left movement would only occur after percolation was complete. For $3 \times m$ nanosensors with ETL structure there are opportunities for the electrical current to move right to left before percolation

completes, however these opportunities create redundancy. Right to left movement would either occur after percolation was complete or would take the electrical current back to the left contact.

In general when the electrical current can move in all directions, the reliability functions and expected lifetimes of $n \times m$ sized nanosensors will be the same as or higher than when movement is restricted. To see the difference between the two scenarios we use the following algorithm, which is a slight modification of the algorithm proposed in [5–7]. Here we use the algorithm to obtain estimates for the exact value of the reliability function and expected lifetime when the electrical current can move in all directions.

Algorithm to Simulate the Lifetime of a Nanosensor

1. A chosen lattice (SL, ETL, or HL) is generated.
2. Under each model a sequence of iid Bernoulli(pi) random variables are generated and assigned to the nanowires to determine their status as functioning or broken during cycle *i*, $i = 1,2,3,...$
3. Any nanowires that break are removed from consideration, and the remaining nanowires are sorted into open clusters (any connected component of the lattice in which all of the nanowires are functioning).
4. The clusters are tested for percolation. If no clusters percolate, then the algorithm is stopped. The result is recorded, and the next simulation starts.
5. If one of the clusters percolates, then the remaining open nanowires are assigned new Bernoulli random variables and steps (c) and (d) are repeated. Example 1 demonstrates the accuracy of our algorithm and presents several cases where there is no increase in reliability or expected lifetime.

Example 1: The lifetime of the nanosensor was simulated 10,000 times for each of three nanosensors with the SL structure for several values of *p*. Figure 3a shows the log of the expected lifetime for these three nanosensors when the electrical current can move in all directions. For comparison, Figure 3b shows the log of the expected lifetime for the same three nanosensors when movement is restricted. As can be seen, there is very little difference between the two Figures. As previously stated, the expected lifetime for the 2×10 nanosensor will be the same in both scenarios. This also allows us to look at the accuracy of our algorithm. Comparing the values for the expected lifetime for the 2×10 nanosensor in both scenarios, we see that our algorithm appears to be accurate. The two figures also show us that the expected lifetimes of the 5×5 and 8×3 sized nanosensors do not benefit from the electrical current moving in all directions. Similarly, the reliability functions do not benefit either. Figure 4a shows the reliability function for the 5×5 nanosensor for both scenarios when $p = 0.95$. Since the difference between the two functions is not discernible, we have plotted the differences in Figure 4b. They are all very close to zero. We repeated this example for three nanosensors with ETL structure and for three nanosensors with HL structure. Comparing the two scenarios we again see that with smaller sized nanosensors there is little difference in the expected lifetimes. See Figures 5a–6b.

In general, we find that larger nanosensors benefit more from the electrical current moving in all directions. This is due to the fact that allowing the electrical current to move right to left creates more percolation paths when the nanosensor is larger. Example 2 provides a rational for this claim, while

Example 3 illustrates two scenarios where the reliability of a nanosensor increases when the electrical current can move in all directions.

Figure 3. *log* $E(X_{n \times m})$ calculated using our algorithm for various values of n and m when (**a**) the electrical current can move in all directions and when (**b**) movement is restricted.
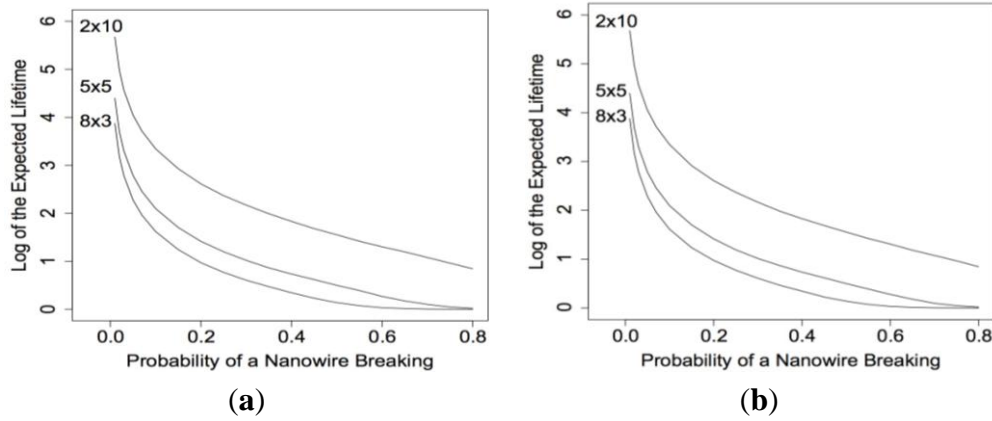

(**a**)   (**b**)

Figure 4. (**a**) $R_{5 \times 5}(x)$ calculated using our algorithm when the electrical current can move in all directions and when movement is restricted when $p = 0.95$ and (**b**) the difference between the $R_{5 \times 5}(x)$.
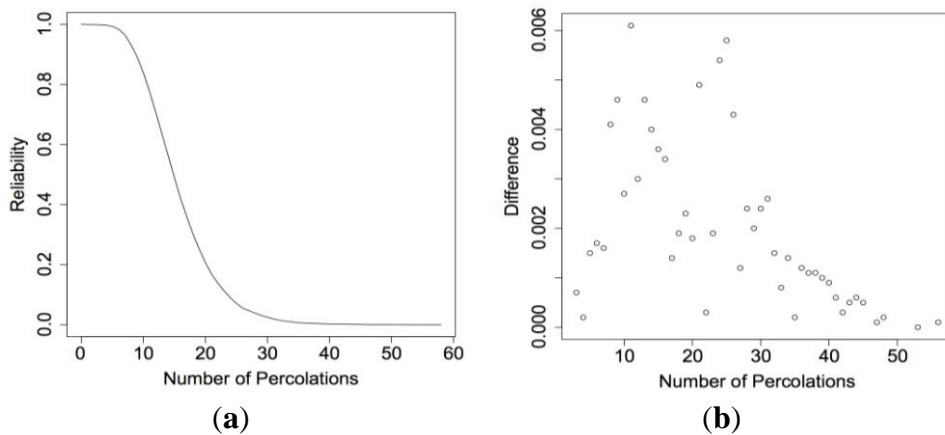

(**a**)   (**b**)

Figure 5. *log* $E(X^{E}_{n \times m})$ calculated using our algorithm for various values of n and m when (**a**) the electrical current can move in all directions and when (**b**) movement is restricted.
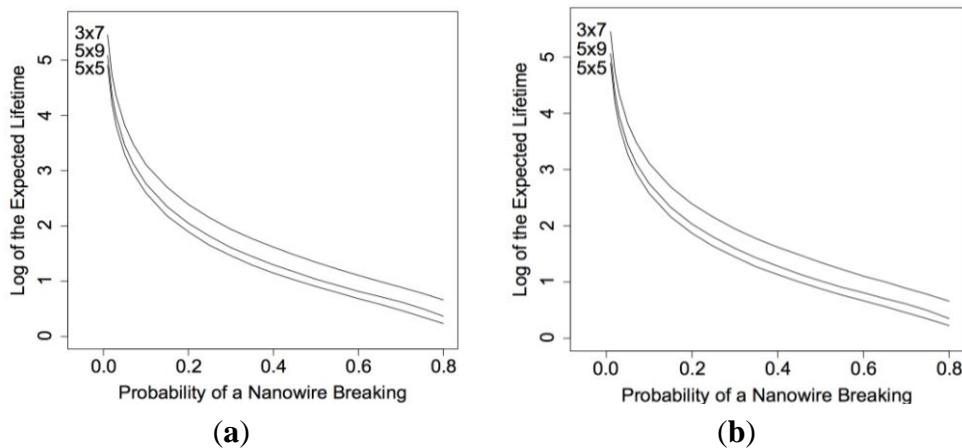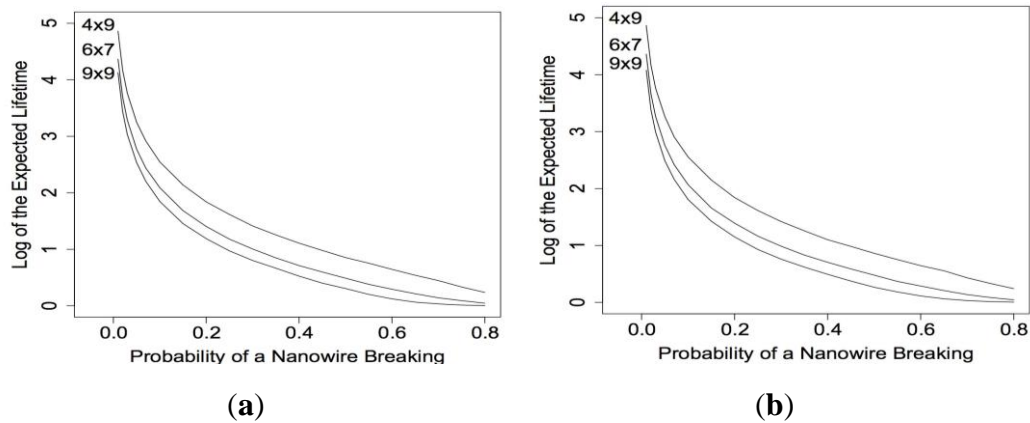

(**a**)   (**b**)

Figure 6. *log E($X^H_{n \times m}$)* calculated using our algorithm for various values of *n* and *m* when (**a**) the electrical current can move in all directions and when (**b**) movement is restricted.


(**a**) (**b**)

Example 2: Consider the 5 × 5 nanosensor with ETL structure shown in Figure 7. The nanowires drawn with dashed lines do not create new percolation paths when the electrical current is allowed to move right to left. Right to left movement through the dashed nanowires would occur after percolation was complete, cause the current to return to the left contact, or cause the percolation path to unnecessarily form a loop on itself. Only the solid nanowires can create new percolation paths. However, the nanosensor will percolate without requiring the electrical current to move right to left in most cases. So the 5 × 5 nanosensor with ETL structure will not have as much of an increase in reliability as a larger nanosensor would.

Figure 7. 5 × 5 nanosensor with ETL structure. Dashed lines do not benefit percolation when the electrical current can move in all directions.
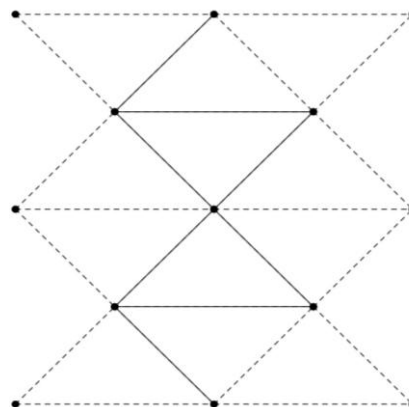

Example 3: Consider a 10 × 10 and a 20 × 20 nanosensor with SL structure. Figure 8a shows the reliability functions for the 10 × 10 nanosensor when *p* = 0.90 for both scenarios. The dashed line represents the reliability when the electrical current can move in all directions. Here we begin to see a slight increase in the reliability. The largest increase occurs when *x* = 6, where the difference between the two reliability functions is 0.0225. Since the differences are still hard to discern, we plotted the differences in Figure 8b. The expected lifetime for the 10 × 10 nanosensor when *p* = 0.90 is 7.3737 when the electrical current can move in all directions and 7.2985 when movement is restricted. Even though the reliability increased, the expected lifetime did not significantly change.

Figure 8. (**a**) $R_{10 \times 10}(x)$ calculated using our algorithm when the electrical current can move in all directions (top curve) and when movement is restricted (bottom curve) when $p = 0.90$ and (**b**) the difference between the $R_{10 \times 10}(x)$.

(**a**) (**b**)
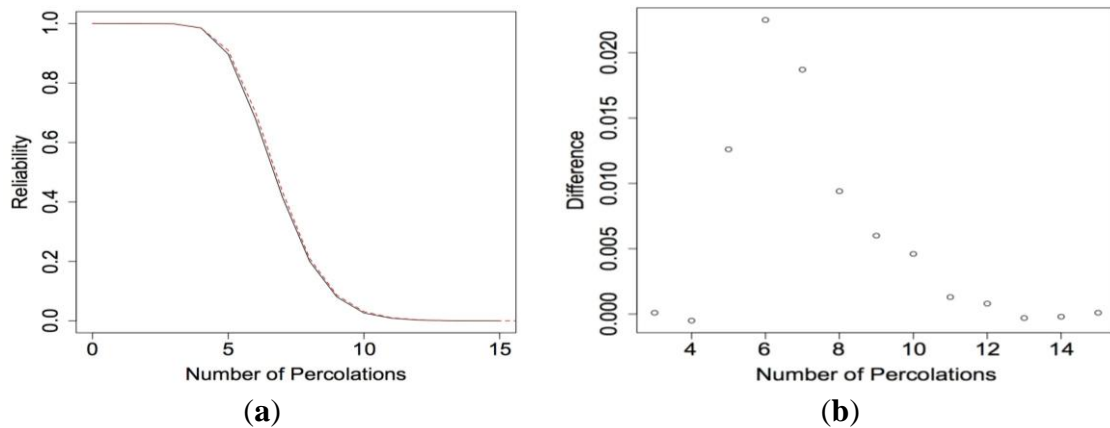
Next, Figure 9a shows the reliability functions for the 20×20 nanosensor when $p = 0.90$ for both scenarios. With the increase in the size of the nanosensor, the increase in reliability becomes more obvious. When $x = 32$ the reliability increases by 0.0754. This is quite a large increase. Furthermore, we find that the increase in reliability is even larger for larger values of p. See Figure 10a for the reliability functions for the 20×20 nanosensor when $p = 0.98$. Here the largest increase in reliability is 0.0909. The expected lifetime for the nanosensor when $p = 0.98$ is 35.3291 when the electrical current can move in all directions and 34.4678 when movement is restricted. Again, although the reliability increased, the expected lifetime did not change as significantly.

Figure 9. (**a**) $R_{20 \times 20}(x)$ calculated using our algorithm when the electrical current can move in all directions (top curve) and when movement is restricted (bottom curve) when $p = 0.90$ and (**b**) the difference between the $R_{20 \times 20}(x)$.

(**a**) (**b**)
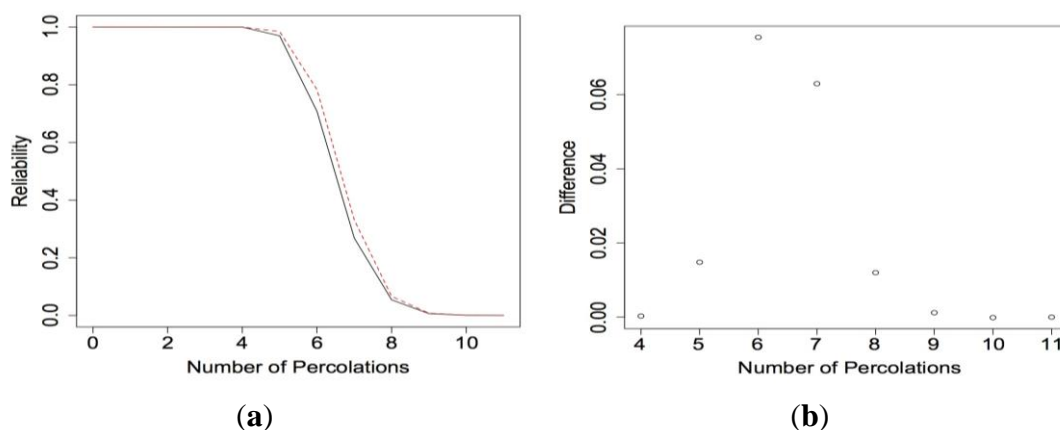
We can also show that a significant increase in reliability occurs for nanosensors with ETL and HL structures of larger sizes. Figure 11a shows the reliability functions for a 21×21 nanosensor with ETL structure when $p = 0.95$, and Figure 12a shows the reliability functions for a 9×9 nanosensor with HL structure when $p = 0.90$. For both figures the dashed lines represent the reliability when the electrical current can move in all directions.

Figure 10. (**a**) $R_{20 \times 20}(x)$ calculated using our algorithm when the electrical current can move in all directions (top curve) and when movement is restricted (bottom curve) when $p = 0.98$ and (**b**) the difference between the $R_{20 \times 20}(x)$.
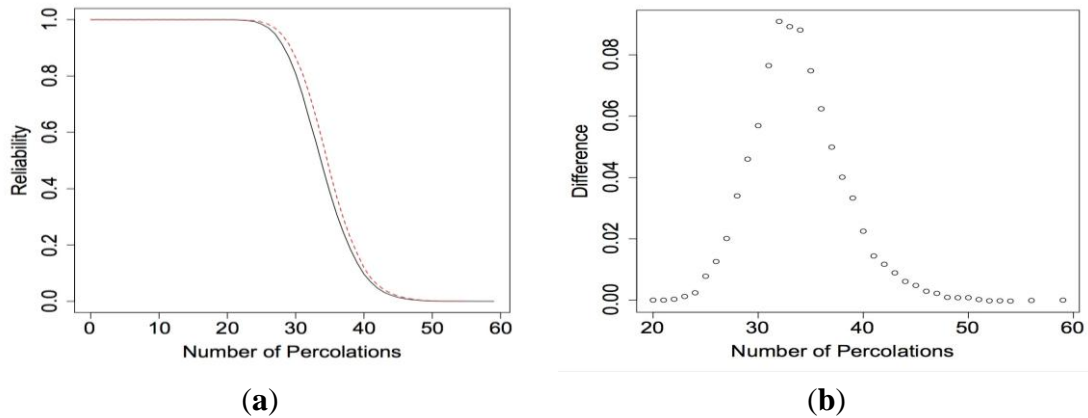

(**a**)   (**b**)

Figure 11. (**a**) $R^E_{21 \times 21}(x)$ calculated using our algorithm when the electrical current can move in all directions (top curve) and when movement is restricted (bottom curve) when $p = 0.95$ and (**b**) the difference between the $R^E_{21 \times 21}(x)$.

(**a**)   (**b**)
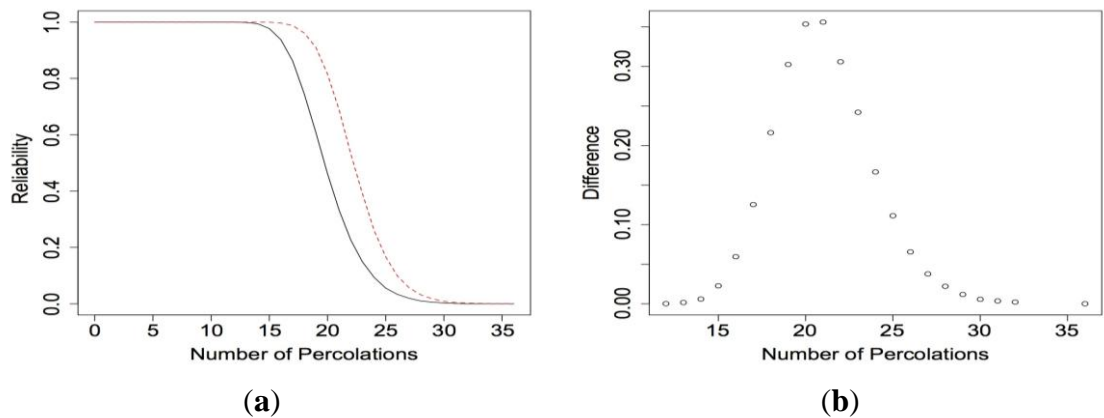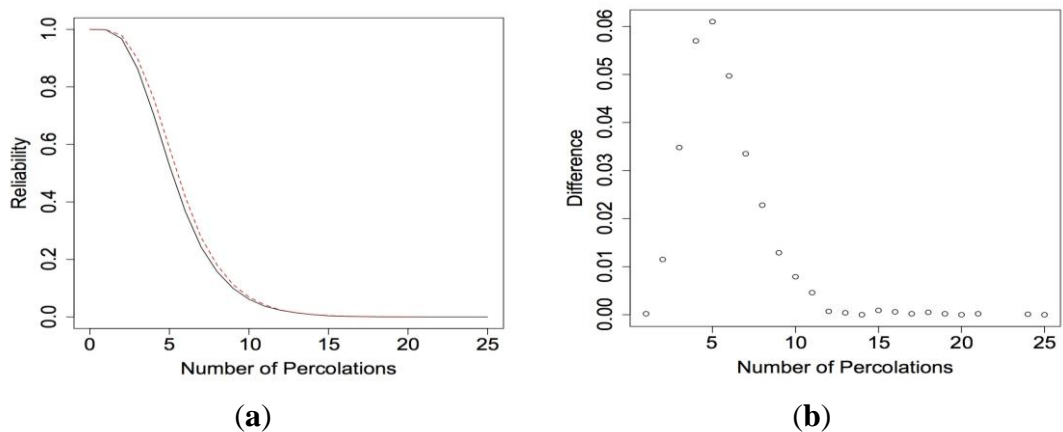
Figure 12. (**a**) $R^H_{9 \times 9}(x)$ calculated using our algorithm when the electrical current can move in all directions (top curve) and when movement is restricted (bottom curve) when $p = 0.90$ and (**b**) the difference between the $R^H_{9 \times 9}(x)$.

(**a**)   (**b**)

2.2. Model 2: Dynamic p

In [6] and [7] the authors presented exact formulas for the reliability functions and expected lifetimes for $2 \times m$ nanosensors with SL structure, $3 \times m$ nanosensors with ETL structure, and $4 \times m$ nanosensors with HL structure operating in dynamic environments. These formulas still hold when the electrical current can move in all directions. For general $n \times m$ nanosensors under Model 2, we experience the same phenomena as in Model 1: the reliability increase is more substantial for larger sized nanosensors when the electrical current can move in all directions. Examples 4 and 5 support this claim.

Example 4. Using the algorithm presented in Section 2.1 we simulated the lifetime of the nanosensor 10,000 times for a 5×5 nanosensor with SL structure, a 5×15 nanosensor with ETL structure, and a 6×13 nanosensor with HL structure. We assumed that these nanosensors were operating under uniform decay. Mathematically, we let $log(p_i/p_{i-1}) = -\beta$, $i = 2,3,4,...$ Equivalently, $p_i = p_{i-1}e^{-\beta}$, $i = 2,3,4,...$ Here β is the non-negative uniform decay factor. For the 5×5 nanosensor with SL structure and the 6×13 nanosensor with HL structure, we let $\beta = 0.01$. For the 5×15 nanosensor with ETL structure, we let $\beta = 0.005$. Figure 13a shows the log of the expected lifetimes for these nanosensors for several values of p_1. For comparison, Figure 13b shows the log of the expected lifetimes when the movement of the electrical current is restricted. The nanosensors in this example are too small to benefit from the electrical current being able to move right to left, so there is little difference between the two figures.

Figure 13. *log $E(X_{5 \times 5})$, log $E(X^E_{5 \times 15})$, and log $E(X^H_{6 \times 13})$* calculated using our algorithm when $\beta = 0.01$, $\beta = 0.005$, and $\beta = 0.01$, respectively when (**a**) the electrical current can move in all directions and when (**b**) movement is restricted.

(**a**)   (**b**)
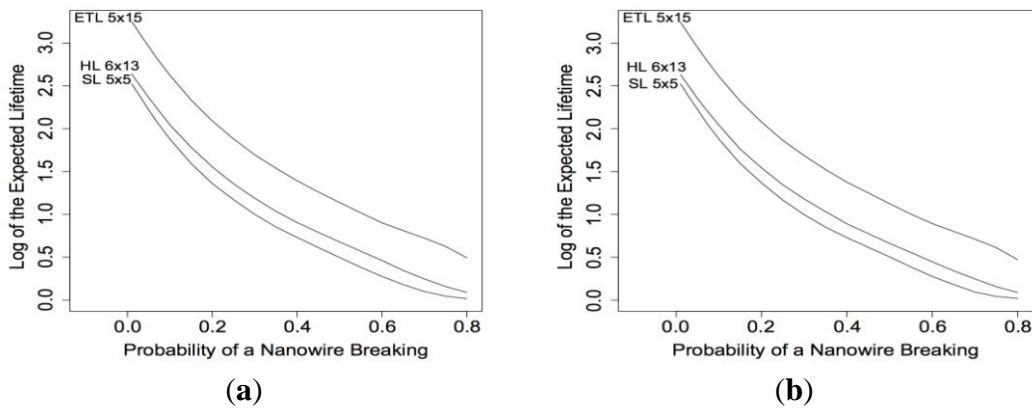
Example 5. We examined the reliability functions for three nanosensors with different structures operating under uniform decay. Figure 14a shows the reliability functions for a 3×5 nanosensor with SL structure when $p_1 = 0.90$ and $\beta = 0.01$ for both scenarios. For this specific nanosensor the reliability functions are exactly the same. So we can use this example to assess the accuracy of our algorithm under Model 2. The differences between the two reliability functions are shown in Figure 14b. The differences are very small, so we conclude that our algorithm works well. Next Figure 15a shows the reliability functions for a 7×13 nanosensor with ETL structure when $p_1 = 0.95$ and $\beta = 0.01$. The reliability increases by as much as 0.0741 when the electrical current can move in all

directions. However, the expected lifetime only increases from 13.26 to 13.57. Figure 16a shows the reliability functions for a 7×5 nanosensor with HL structure when $p_1 = 0.98$ and $\beta = 0.005$. Here the reliability increases by as much as 0.0218.

Figure 14. (**a**) $R_{3 \times 5}(x)$ calculated using our algorithm when the electrical current can move in all directions (top curve) and when movement is restricted (bottom curve) when $p_1 = 0.90$ and $\beta = 0.01$ and (**b**) the difference between the $R_{3 \times 5}(x)$.
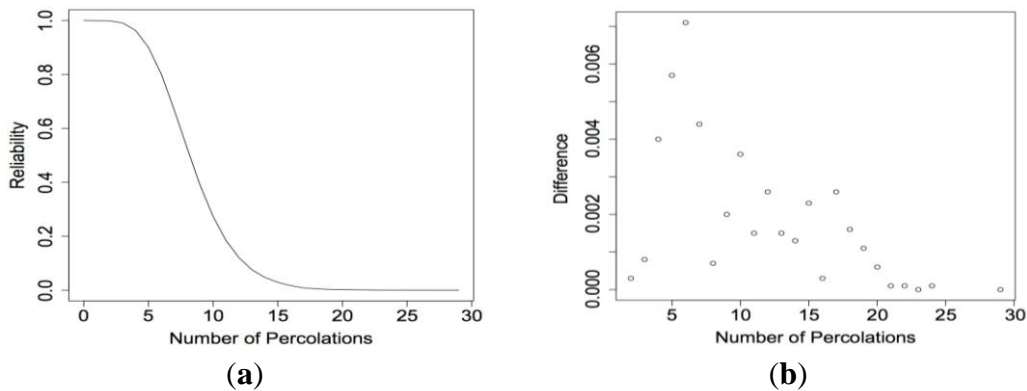

(**a**)   (**b**)

Figure 15. (**a**) $R^{E}_{7 \times 13}(x)$ calculated using our algorithm when the electrical current can move in all directions (top curve) and when movement is restricted (bottom curve) when $p_1 = 0.95$ and $\beta = 0.01$ and (**b**) the difference between the $R^{E}_{7 \times 13}(x)$.
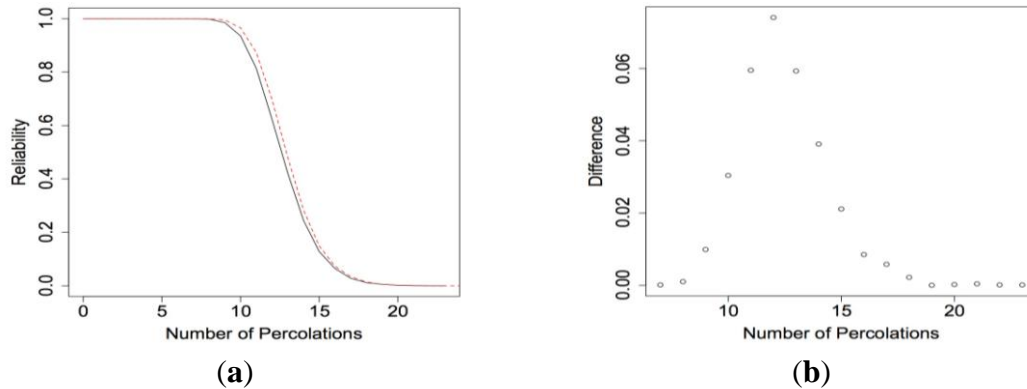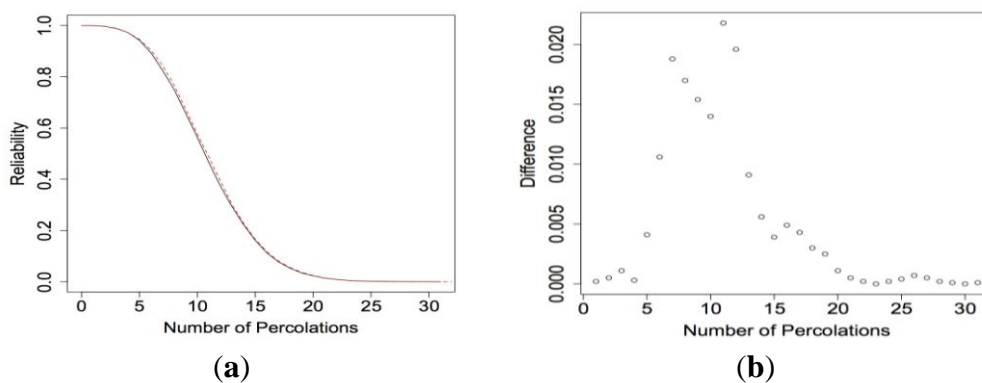

(**a**)   (**b**)

Figure 16. (**a**) $R^{H}_{7 \times 5}(x)$ calculated using our algorithm when the electrical current can move in all directions (top curve) and when movement is restricted (bottom curve) when $p_1 = 0.98$ and $\beta = 0.005$ and (**b**) the difference between the $R^{H}_{7 \times 5}(x)$.

(**a**)   (**b**)

3. Theoretical Properties of the Reliability Growth

In this section we provide several properties of the increase in reliability that occurs for our nanosensor when the electrical current can move in all directions. Suppose $X(AD)$ denotes the number of cycles of H_2 that our nanosensor will withstand when the electrical current can move in all directions (AD) and $X(R)$ denotes the number of cycles when movement is restricted (R). It is clear that we have the following relationship.

$$X(AD) =^{st} X(R)+W, \tag{1}$$

where st stands for stochastic. That is, the number of cycles when the electrical current can move in all directions is stochastically equal to the number of cycles when movement is restricted plus some non-negative integer random variable W.

From Equation (1) the reliability of our nanosensor when the electrical current can move in all directions, $R_1(x) = P(X(AD) > x)$, can be written as

$$R_1(x) = P(X(AD) > x) = P(X(R)+W > x)$$
$$= \sum_{z=0}^{x} P(X(R)=z)+P(X(R) > x) \tag{2}$$
$$= \sum_{z=0}^{x} P(W > x\text{-}z)P(X(R)=z)+R_2(x),$$

where $R_2(x) = P(X(R) > x)$ is the reliability function of our nanosensor when movement is restricted. Now using Equation (2), we obtain an expression for the difference between the two reliability functions, which we refer to as the reliability growth $H(x)$.

$$H(x) = R_1(x) - R_2(x) = \sum_{z=1}^{x} P(W > x\text{-}z)a_z, \tag{3}$$

where $a_z = P(X(R) = z)$. Note that $a_0 = P(X(R) =0) = 0$.

The following Theorem gives the bound for $H(x)$, the reliability growth.

Theorem 1. $0 \leq H(x) \leq E(W)a(x)$, where $a(x) = max(a_1, a_2,..., a_x)$.

Proof. Using Equation (3), we have
$$H(x) = \sum_{z=0}^{x} P(W > x\text{-}z)a_z$$
$$\leq \sum_{z=0}^{x} P(X > x\text{-}z)a(x)$$
$$\leq E(W)a(x).$$
The second inequality comes from the fact that $E(W) = \sum_{w=0}^{\infty} P(W > w)$.

In Theorem 1 if $E(W) = 0$, then $H(x) = 0$, which represents no reliability growth. For an example of $H(x) = 0$ consider the 2×10 nanosensor with SL structure from Example 1.

To state our next result, which compares two nanosensors with different sizes and/or structures, we need the following definition and notations.

Definition 1. For any discrete random variable X, the reverse hazard function is $h(x) = P(X=x) / P(X \leq x)$. For more details see Shaked and Shanthikumar [9].

Now let $p(i)$ be the probability of a nanowire not breaking for nanosensor i, $i = 1,2$. Also let $H_i(x)$ be the reliability growth for nanosensor i, $i = 1,2$, and let i, $X_i(R)$ be the discrete random variable for nanosensor i, $i = 1,2$, when the movement of the electrical current is restricted. Then $h_i(x)$ is the reverse hazard function for $X_i(R)$ for nanosensor i, $i = 1,2$. Then we have the following result.

Theorem 2. If $p(1) < p(2)$ and $h_1(x) < h_2(x)$, then $H_2(x)/H_1(x) \geq P(X_2(R) \leq x)/P(X_1(R) \leq x)$.

Proof. From Equation (3) we have

$$H_2(x) = \sum_{z=0}^{x} P(W_2 > x-z)P(X_2(R) = z)$$
$$\geq \sum_{z=0}^{x} P(W_1 > x-z)P(X_2(R)=z)$$
$$\geq [P(X_2(R) \leq x)/P(X_1(R) \leq x)]\sum_{z=0}^{x} P(W_1 > x-z)P(X_1(R) = z)$$
$$= [P(X_2(R) \leq x)/P(X_1(R) \leq x)]H_1(x).$$

To see how good this bound is consider the following example.

Example 6. Consider a 12×17 nanosensor with SL structure. Let $p(1)=.85$ and $p(2) = 0.90$. Using $p(1)$ we have $h_1(7) = 0.0508$, and using $p(2)$ we have $h_2(7) = 0.6528$. So $p(1) < p(2)$ and $h_1(7) < h_2(7)$. Thus by Theorem 2 we have $H_2(7)/H_1(7) \geq 0.4759$. Next we compare our 12×17 nanosensor when $p(1) = 0.85$ to a 10×15 nanosensor with SL structure when $p(2) = 0.90$. For the 12×17 nanosensor we have $h_1(5) = 0.7144$. For the 10×15 nanosensor $h_2(5) = 0.9662$. Then by Theorem 2 we have $H_2(7)/H_1(7) \geq 0.0300$.

4. Conclusions

In this paper we investigated the reliability of a specific hydrogen gas nanosensor made from a network of palladium nanowires. We assumed that the electrical current could move in all directions. This work is an extension of [5–7], where we assumed that the electrical current could not move right to left, *i.e.*, movement was restricted. We find that allowing the electrical current to move in all directions results in a higher reliability and expected lifetime for our nanosensor. We presented several examples that support this claim, and we showed that larger sized nanosensors experience a larger increase in reliability. This holds true for all structures that we used to model the nanosensor and for both models that we presented for the probability of a nanowire not breaking. We also presented an algorithm, which is a modification of the algorithm originally presented in [5], to simulate the lifetime of the nanosensor when the electrical current can move in all directions.

Acknowledgments

Conflict of Interest

The authors declare no conflict of interest.

References

1. Zeng, X.Q.; Latimer, M.L.; Xiao, Z.L.; Panuganti, S.; Welp, U.; Kwok, W.K.; Xu, T. Hydrogen gas sensing with networks of ultrasmall palladium nanowires formed on filtration membranes. *Nano Lett.* **2011**, *11*, 262–268.
2. Zeng, X.Q.; Wang, Y.L.; Deng, H.; Latimer, M.L.; Xiao, Z.L.; Pearson, J.; Xu, T.; Wang, H.H.; Welp, U.; Crabtree, G.W.; *et al.* Networks of ultrasmall Pd/Cr nanowires as high performance hydrogen sensors. *ACS Nano* **2011**, *5*, 7443–7452.
3. Zeng, X.Q.; Wang, Y.L.; Xiao, Z.L.; Latimer, M.L.; Xu, T.; Kwok, W.K. Hydrogen responses of ultrathin Pd films and nanowire networks with a Ti buffer layer. *J. Mater. Sci.* **2012**, *47*, 6647–6651.
4. Yang, F.; Taggart, D.K.; Penner, R.M. Fast, sensitive hydrogen gas detection using single palladium nanowires that resist fracture. *Nano Lett.* **2009**, *9*, 2177–2182.
5. Ebrahimi, N.; McCullough, K.; Xiao, Z. Reliability of sensors based on nanowire networks. *IEEE Trans. Nanotechnol.* **2013**, *45*, 215–228.
6. Ebrahimi, N.; McCullough, K.; Xiao, Z. Reliability of sensors based on nanowire networks operating in a dynamic environment. *IEEE Trans. Reliab.* **2013**, *62*, 908–916.
7. Ebrahimi, N.; McCullough, K.; Xiao, Z. Reliability of sensors based on nanowire networks modeled by equilateral triangle and hexagonal lattices. *IEEE Trans. Nanotechnol*. **2013**, *1*, 81–95.
8. Masuda, H.; Ashoh, H.; Watanabe, M.; Nishio, K.; Nakao, M.; Tamamura, T. Square and triangular nanohole array architectures in anodic alumina. *Adv. Mat.* **2001**, *13*, 189–192.
9. Shaked, M.; Shanthikumar, J.G. *Stochastic Orders*; Springer: New York, NY, USA, 2006.